Model of spatiotemporal dynamics of stick-slip motion

B. Lin* and P. L. Taylor
Department of Physics, Case Western Reserve University, Cleveland, Ohio 44106
(Received 9 November 1993)

We propose a model of spatiotemporal dynamics that, in contrast to many earthquake models, does not contain a velocity-weakening frictional force. Dissipation in this model occurs only through viscous forces acting in the presence of a nondissipative random potential. Both small localized and large delocalized events are observed. The scaling behavior of the event probability distribution is found to be nonuniversal and distinct from that found in earthquake models. The system loses instability as the strength of the pulling spring becomes large enough. It also shows transitions from behavior exhibiting a wide range of magnitudes of slipping events to showing a narrow range scale in which only large events occur for a certain range of parameters. Effects of varying system size, boundary conditions, and pulling speed were investigated. Most of our numerical results are in qualitative agreement with the rubber-sheet experiments of Vallette and Gollub [Phys. Rev. E **47**, 820 (1993)].

PACS number(s): 05.40.+j, 91.30.Dk, 05.45.+b, 62.20.Mk

I. INTRODUCTION

The dynamics of slipping has been a topic of both theoretical and experimental interest in recent years [1–6], partly due to its relationship to the concept of self-organized criticality [7] and partly due to its possible relevance to earthquake dynamics. Slipping events in many systems are observed to have event sizes spanning a wide range of magnitudes. In contrast to the situation in equilibrium statistical mechanics, special values of parameters are not necessary in order to observe wide-range critical fluctuations.

This type of phenomenon has been observed in many dynamic systems. A simple deterministic block-spring earthquake model has been proposed by Burridge and Knopoff [8] and studied extensively by Carlson, Langer, and co-workers [1,2], who found numerically a universal power-law distribution for a wide range of magnitudes of slipping events. Slipping experiments that studied granite on granite at large normal forces [3], sandpaper on carpet [4], and rubber sheet on a glass rod [5] have all shown behavior in which a large-range scale of slipping events occurred. The same large-range-scale critical fluctuations exist in lattice and cellular automata models [7,9,10], and sandpile systems [11,12].

In many mechanical models of blocks and springs, such as the Burridge-Knopoff model and its variants [1,13,14], the most important feature responsible for the stick-slip dynamics is the presence of a frictional force $F(\dot{x})$ whose strength becomes weaker as the velocity increases [1],

$$F(\dot{x}) = \frac{-F_0 \,\mathrm{sgn}(\dot{x})}{1+|\dot{x}|} \ , \tag{1}$$

where $\dot{x}$ is the velocity of a block and F_0 is a constant. This nonlinear friction function is the source of the stick-slip instability. Numerical calculations in Refs. [1] and [2] indicate that the event probability distributions obey certain scaling laws. For large dissipation, the probability $P(\mu)$ of an event of magnitude μ occurring has the form

$$P(\mu) \simeq \begin{cases} Ae^{-b\mu} \ , & \mu < \mu_0 \\ A'e^{-b'\mu} \ , & \mu > \mu_0 \end{cases} \tag{2}$$

with $b \approx 0.95$ and $b' \approx -1$, where A is a constant and μ_0 the crossover magnitude dividing the regions of small and large events. For small enough dissipation, the event probability roughly shows a single scaling

$$P(\mu) \simeq Be^{-b''\mu} \ , \tag{3}$$

with $b'' \approx 0.35$ and B a constant.

Another type of block-spring earthquake model was recently proposed and studied by Knopoff and co-workers [14]. In their model the velocity-weakening aspect of the frictional force was introduced through the presence of separate sticking and sliding coefficients of friction. The coefficient of sticking friction varied randomly from block to block, and a viscous force was also used.

Vallette and Gollub [5] recently conducted an experiment on the dynamics of slipping and have found some interesting results. They used a stretched thin rubber sheet pressed against a long cylindrical glass rod, and translated the rod at a constant speed. Digitized optical measurement of the one-dimensional displacement and event distributions of the rubber-sheet system showed a broad distribution of event sizes, similar to the behavior in earthquake models. There are, however, two major differences between results in the rubber-sheet system and in earthquake models. The friction between the rubber

*Present address: Department of Physics, University of Minnesota, Minneapolis, MN 55455.

sheet and the glass rod was measured and found to be velocity strengthening instead of velocity weakening as employed in earthquake models. Also, the scaling behavior for event distribution measured in the rubber-sheet system did not always agree with the predictions of the earthquake models; in particular, they found that in contrast to earthquake models, the scaling exponent b for small events decreases as dissipation increases.

Vallette and Gollub's experiment suggests that there is an alternative mechanism for stick-slip dynamics. They argued that the instability in their experimental system is due to local detachment of the elastic sheet from the glass rod. The discrepancy between the scaling behavior measured in the rubber sheet and calculated from earthquake models also raises an interesting question: is there a universal scaling law governing all stick-slip dynamics? Or is the scaling dependent on the details of the models considered?

In this paper we propose an alternative one-dimensional mechanical model and describe some theoretical and computer-simulation studies designed to answer the question of scaling universality. The block-spring model studied in this paper is similar in some respects to previous earthquake models, but differs from them in its lack of any frictional force term in the equations of motion. Instead, a random Gaussian potential that acts on the blocks mimics the hills and valleys of a rough surface. This nondissipative force is supplemented by a viscous force that adds the necessary dissipation to the model. While the model has in common with Ref. [13] the presence of a stochastic element, it differs from it and from most previous models in the absence of any velocity-weakening frictional force. The viscous force, which is the only nonconservative element in our model, is of course velocity strengthening. We will calculate the displacement of blocks, their velocities, and the time distribution of events in order to study spatial and temporal dynamics, and study the event probability distribution in order to examine the scaling law. We will also analyze the dependence of the dynamics on system size, minimum event size, and pulling speed.

II. THE MODEL

The one-dimensional model we will study is depicted schematically in Fig. 1. The N blocks of mass m are connected in a chain by Hookean springs of force constant s_1. Each block is attached to a rigid body moving at a constant velocity v (the pulling speed) via Hookean springs of force constant s_2. The blocks are pulled on a fixed rough surface whose interaction with the blocks is represented by a random Gaussian potential $G(x)$,

$$G(x) = -\frac{k}{2d}\sum_l R_l\, e^{-d(x-l)^2}, \tag{4}$$

where the l are integers, k is the depth parameter of the potential, and d is the width parameter, and the R_l random numbers between 0 and 1. We have taken the

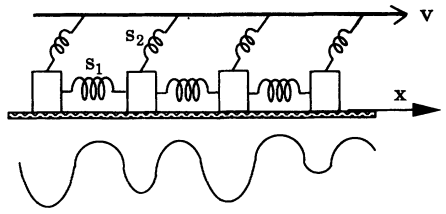

FIG. 1. Illustration of the one-dimensional block-spring model.

equilibrium spacing between two blocks to be unity, and chose d sufficiently large to make the results independent of its actual magnitude. The frictional force that was described in terms of a macroscopic coefficient of friction in other models is now replaced by the effects of the random potential $G(x)$, and so does not appear in our model. All energy dissipation then occurs solely through a viscous-force term of the same form as was present in the model of Burridge and Knopoff [8].

The equations of motion for this model system are

$$m\frac{d^2x_i}{dt^2} = s_1(x_{i+1} - 2x_i + x_{i-1}) + s_2[vt - (x_i - i)] - k\sum_{l=-\infty}^{+\infty} R_l(x_i - l)e^{-d(x_i-l)^2} - \gamma\frac{dx_i}{dt}, \quad i = 1, 2, \ldots, N, \tag{5}$$

where γ describes the strength of the viscous force. The mass m will be taken as unity in our discussion throughout this paper. We investigate the effects of the five independent parameters in Eq. (5): s_1, s_2, v, k, and γ. We shall assume an initial configuration of blocks of either a uniform distribution

$$x_i = i, \tag{6}$$

or a spatially nonuniform configuration with each block deviating randomly by a small amount from its equilibrium position, so that

$$x_i = i + (R_i' - 0.5)\delta. \tag{7}$$

Here R_i' is a random number in (0,1) and δ a small constant, typically 0.1.

Our model (5) differs from that used by Carlson, Langer, *et al.* [1,2] in that a random element is introduced into the equations of motion themselves, and does not arise in a translationally invariant system as a consequence of velocity-weakening friction. The random potential (4) provides an instability mechanism more closely in accord with microscopic tribological considerations: a detachment process occurs when some blocks overcome the potential barriers and start sliding. The linear velocity-dependent term $-\gamma\dot{x}_i$ allows dissipation of the kinetic energy that would otherwise accumulate as work is done by the pulling springs.

III. NUMERICAL CALCULATIONS

The coupled differential equations (5) were solved numerically by use of the standard Runge-Kutta procedure. The system size studied was typically $N = 50$, although some larger variants with N up to 150 were also examined to verify that no qualitative change in behavior would be observed.

The system was always started completely at rest from the positions described by Eq. (6) or (7). Although the stick-slip motion is in general not periodic in time, big slipping events were found to be approximately periodic in time with period $1/v$, as might be expected from the translational invariance of the chain of blocks. The time steps used in the numerical procedure were 0.0002 of this fundamental time unit. We discarded the first 5×10^5 time steps (about 100 cycles of big events) in order to let the system reach a steady state, then collected data for about 10^7 time steps, or about 2200 loading cycles.

A criterion was set for the smallest slipping that would be counted as an event. Since the event size is measured by block displacement, a minimum displacement was defined as the threshold for an event. The size $\Delta x_{\min}$ of this minimum displacement was set arbitrarily as the distance traveled at twice the pulling speed v in one time step Δt,

$$\Delta x_{\min} = 2v\Delta t. \tag{8}$$

As a check on the appropriateness of this criterion, two other $\Delta x_{\min}$ were also studied to see their effect on the scaling behavior of the event probability distribution.

We will calculate various event-related quantities: event distributions in time, space, and size, and velocities of blocks in different events. An event can be defined in a two-dimensional lattice of position and time: if a block at a given (discrete) time has a displacement greater than $\Delta x_{\min}$, that point is marked in the position-time space to have a slipping point. An event is then a cluster of all connected slipping points.

The moment M of an event is defined in the same way as in earthquake models [1],

$$M = \sum_i \Delta x_i, \tag{9}$$

where i is summed over all blocks contained in the event. The magnitude μ of the event is then defined as

$$\mu = \ln M. \tag{10}$$

The event probability distribution $P(\mu)$ is the frequency of events per unit length of μ. We will normalize the number of events per unit μ interval by dividing by the total number of events in the entire run used to obtain $P(\mu)$.

IV. NUMERICAL RESULTS

A. Spatiotemporal dynamics

We observed slipping events of various sizes distributed over space and time. Figure 2(a) shows the block displacements $x_i(t)$. The parameters used in this figure are $s_1 = 30$, $s_2 = 20$, $k = 350$, $d = 50$, $v = 0.015$, and $\gamma = 4.0$. We see both big events (large slipping involving a large number of blocks) and small events (events with small slipping and a small number of blocks), and the time spent in slipping is much less than the time spent in loading. One time unit in the figure is 67 time steps.

Figure 2(b) shows another view of the same spatiotemporal dynamics. Here we plot equal-time contour lines on the $\hat{x}_i(t)$-$x_i(t)$ plane, where the cumulative displacement $\hat{x}_i(t)$ is as defined in Ref. [5],

$$\hat{x}_i(t) = vt + x_i(t). \tag{11}$$

The areas where the lines are dense represent sticking, while the white areas where the lines are widely separated portray slipping events. Only some of the 50 blocks are shown in Fig. 2(a), as we have magnified part of the system to show more clearly the small slipping events. This behavior appears qualitatively similar to that seen in Vallette and Gollub's experiment (Ref. [5]).

The stick-slip dynamics of various event sizes can also be seen by plotting the velocities of the blocks in position and time for this same simulation, as shown in Fig. 3.

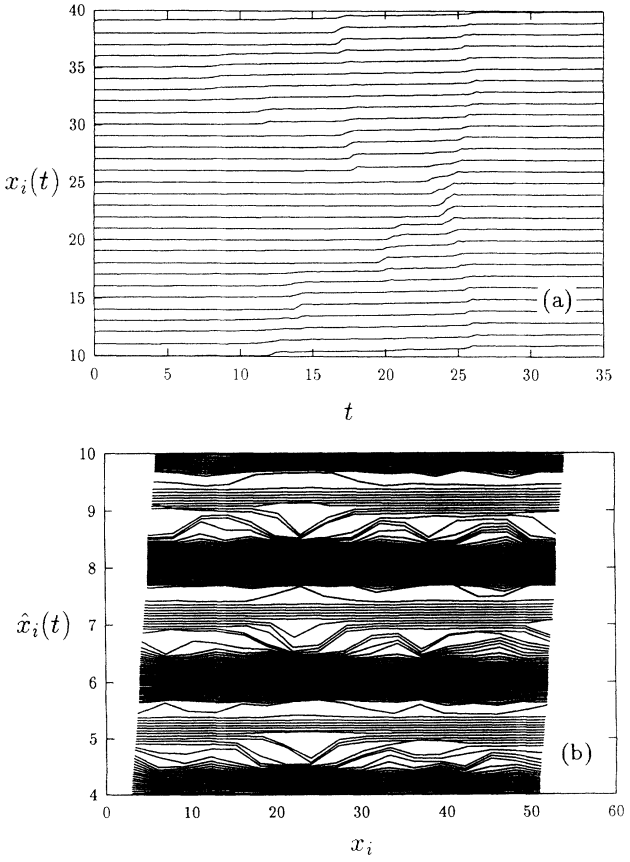

FIG. 2. The model shows a wide range of slipping events. Shown here is a typical system with parameters $s_1 = 30$, $s_2 = 20$, $k = 350$, $d = 50$, $v = 0.015$, and $\gamma = 4.0$. (a) Displacement of blocks as a function of time, (b) equal-time contour map showing the cumulative displacement $\hat{x}_i(t)$ as a function of position and time.

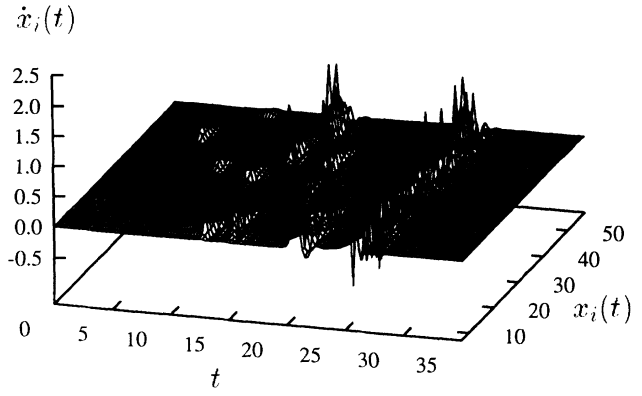

FIG. 3. In this replotting of the data of Fig. 2, the velocities of blocks are shown as a function of position and time. Both localized events with small velocities and big events with large velocities are seen.

Relatively small velocities with a small number of blocks involved in each peak represent small localized slipping events. We note that the pulling speed is $v = 0.015$, and that small events have velocities of the order of v. Also apparent in Fig. 3 are big events involving a large number of blocks and having velocities greater than the pulling speed v by up to two orders of magnitude.

The time distribution of events can be clearly seen in Fig. 4 which displays the size (magnitude μ) of events as a function of time. Even though we impose a minimum displacement for an event to be noted, the range of moments of slipping events spans more than three orders of magnitude. Big events repeat roughly every time interval $1/v$, although the sizes are not the same in each cycle. Small events are less regularly distributed in time and magnitude in each cycle, but tend to group together in time in each cycle. There is a relatively long quiet period of time after big events, and this is shown as a gap between two clusters of events. Each cycle thus begins with quiet creeping motion, and then small events occur, quickly triggering big events.

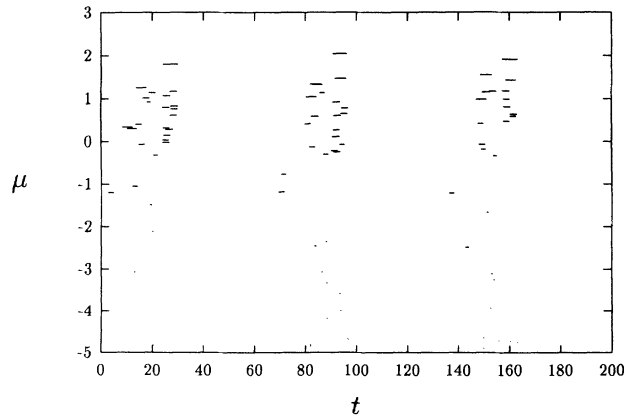

FIG. 4. Time distribution of events. Slipping events form clusters in time. There is a long quiet creeping motion after big events and before the next event cluster.

B. Scaling behavior of the magnitude distribution

We completed a large number of numerical runs in order to study the scaling behavior of the magnitude probability distribution $P(\mu)$ of all events. A typical plot of $\ln P(\mu)$ vs μ is shown in Fig. 5(a), and is very similar to the experimental data reported in Ref. [5]. The curve marked with filled circles in Fig. 5(a) corresponds to a system with relatively small dissipation, $\gamma = 3.0$. Other parameters for this distribution are $s_1 = 60$, $s_2 = 20$, $k = 250$, $d = 50$, $v = 0.015$. We refer to this parameter set as the standard parameter set. For small events the distribution follows the Gutenberg and Richter law [15]

$$P(\mu) = Ae^{-b\mu}, \tag{12}$$

where A is a constant and the scaling exponent b in this case is about 1, which agrees with the predictions of earthquake models [1,2] and with seismological data [15].

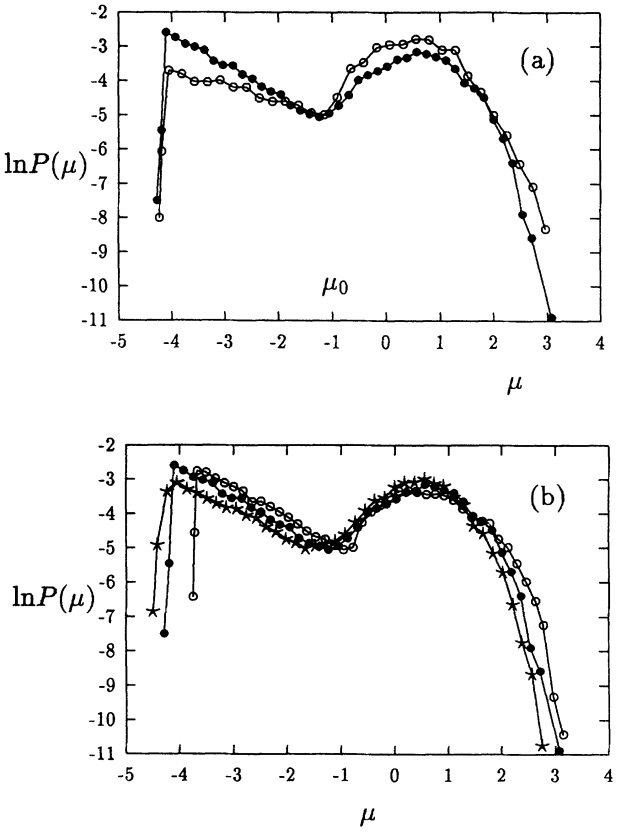

FIG. 5. (a) Logarithm of event probability distribution as a function of magnitude μ. The stronger dissipation (curve with open circles) flattens the distribution in the small-event region. Compared are the system with standard parameter set, $s_1 = 60$, $s_2 = 20$, $k = 250$, $d = 50$, $v = 0.015$, and $\gamma = 3.0$ (filled circles), and the system with $k = 320$ and $\gamma = 5.0$ (open circles). (b) Scaling of distribution is not changed as the interblock spring parameter s_1 is varied. Unlike the case for all the other parameters, however, different s_1 changes crossover magnitude μ_0. All three curves have the same standard parameters except that $s_1 = 30$ for stars, $s_1 = 60$ for filled circles, and $s_1 = 90$ for open circles.

When, however, the dissipation is increased to $k = 320$ and $\gamma = 5.0$, but with the other parameters unchanged, the probability distribution $P(\mu)$ yields a smaller exponent $b \approx 0.65$, as shown by the curve marked with open circles in Fig. 5(a). This contradicts the earthquake models' prediction that weaker dissipation decreases the exponent b. The flatter probability distribution in our model in the small-event regime as dissipation is increased indicates that scattered small slipping events are depressed and less visible and the system's motion is dominated by larger, more concentrated slippings. This type of dependence of motion and probability distribution on dissipation have been reported in the rubber-sheet experiment [5]. The effect of large dissipation on slipping dynamics can also be seen in Fig. 6, the cumulative displacement, which shows large stuck (black) and slipping (white) areas and little small-slipping region.

We also note in Fig. 5(a) that there is no structural change of the distribution when dissipation is decreased, in contrast to the case in earthquake models where the weak-dissipation distribution reduces to one characterized by a single exponent b'' [Eq. (3)]. Except for the cases of very *large* friction or viscosity, where the small-event part of the distribution vanishes (see next section), the distribution curve in our model always shows a pattern of decreasing probability in the small-event region and increasing probability in the large-event region. The absence of a single-scale distribution was similarly observed in the rubber-sheet experiment. We did not attempt to calculate a unique scaling exponent b' to fit Eq. (2) in the large-event region, since that part of the distribution curve is not a good approximation to a straight line. However, a very rough linear fit of the distribution curves from μ_0 to the peak in the positive μ side gives b' a value about 1.5 [Fig. 5(b)].

We do observe in our calculations some scaling behavior that agrees with that found in the earthquake models. The scaling exponent b seems invariant under variation of the parameter s_1 that describes the interblock interaction. Figure 5(b) shows the probability distributions for three different values of s_1, and they all appear to have the same scaling exponent b. Another common feature in scaling behavior is the crossover magnitude μ_0 [Eq. (2), Fig. 5(a)] which marks the crossover from the small-event region scaling to the large-event region scaling, and remains unchanged under variations of all parameters except s_1, in the regions we have studied. The probability distributions in Figs. 5(a), 9, and 10 have different parameters, but show the same crossover magnitude $\mu_0 \approx -1$. When the interblock interaction parameter s_1 is changed, however, μ_0 changes. As shown in Fig. 5(b), the probability distribution with small s_1 has a smaller crossover magnitude than that with larger s_1, and the distribution curve is shifted to the small-μ side when s_1 is decreased. A smaller s_1 thus has more small events but fewer large events than does a larger s_1 because the stiffer pulling springs eliminate smaller slipping events.

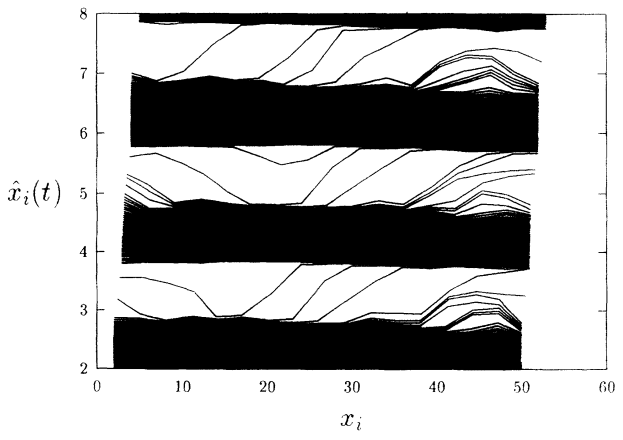

FIG. 6. Cumulative displacement for a system with strong dissipation. Parameters are the same as for the flatter curve in Fig. 5(a). Few small events are visible, and the system is predominantly in either the stuck or the large-slipping state.

To test system size effects, we have also run calculations on systems with size $N = 100$ and $N = 150$. We obtained the same scaling exponent b for the parameters used in the smaller system with $N = 50$. Except for a greater total event number, no difference was found between the large and small systems. This indicates that the self-organized criticality in our model is not an artifact of the finite size. In particular, the rapid decrease in the probability distribution for events of magnitude $\mu > 3$ does not reflect any limitation imposed by the size of the system studied. For example, an event in which each block in a chain of 150 blocks moves by only one lattice spacing would have an event magnitude of $\mu > 5$. The almost complete absence of such events in our simulation is a further indication that size effects were not important.

C. Loss of instability and transition of distribution

The pulling springs s_2 in our model are an abstraction of the effects of the shear modulus of the rubber sheet in Vallette and Gollub's experiment. Increasing s_2 reduces the relative effectiveness of cooperative motion in the chain, and hence is equivalent to reducing the width of rubber sheet in contact with the pulling rod in the experiment. A loss of instability was observed in the experiment [5] as the width of the sheet was substantially reduced, and we find the same phenomenon to occur in our model calculations when the parameter s_2 is substantially increased. Figure 7 shows one such system. All the parameters are the same as those in Fig. 5(a) (i.e., the standard set of parameters) except that $s_2 = 100$. In this case, big events disappear, leaving the event distribution in a narrow range of event size [Figs. 7(a) and 7(b)]. The prominent high-velocity large slips are replaced by a quiet creeping motion with a velocity of the order of the pulling speed [Fig. 7(c)].

By changing some of the other parameters of our model, we can also show transition of dynamical motion to one without small events. This loss of small events can be induced by increasing either the potential or the viscosity. Large static friction (large k) prevents some

small events from occurring since the local stress for these blocks is not large enough to overcome the high potential barrier. A stronger dissipation (large γ) reduces the magnitude of small events and makes them undetectable (smaller than the minimum magnitude for an event). Figure 8 shows the event probability distribution $P(\mu)$ for two cases inside this regime where no small events occur. For large k (normal γ) or large γ (normal k) the distribution shows that only large events are formed. If both k and γ are increased the transition occurs at smaller values than needed for either k or γ alone since the two effects are cumulative.

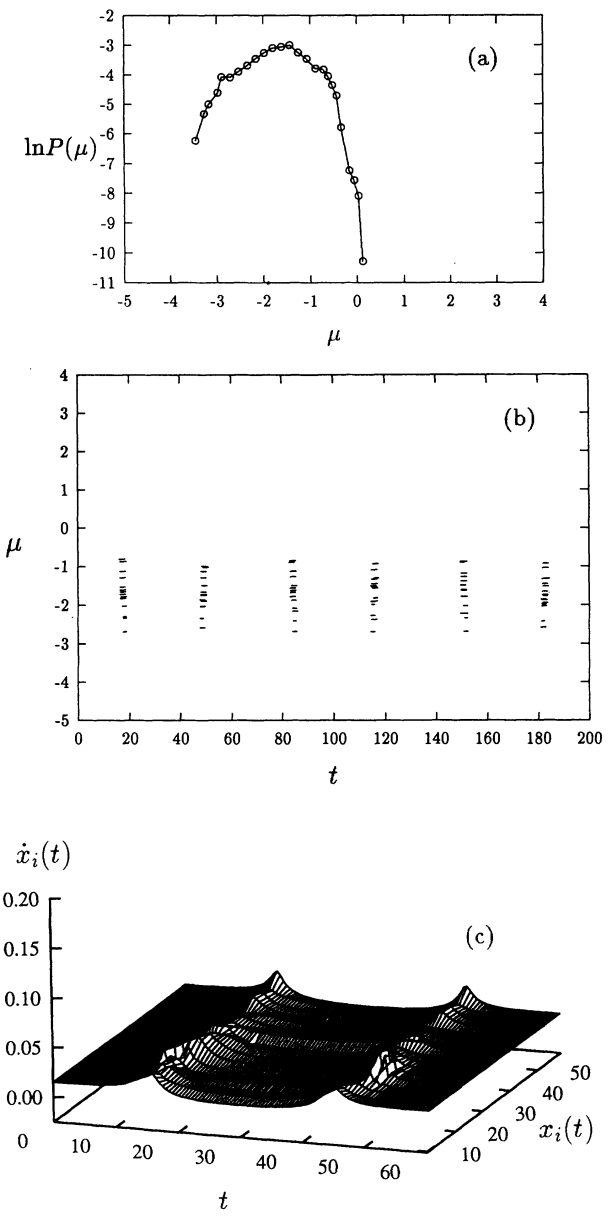

FIG. 7. System loses instability when the parameter s_2 is sufficiently large. Essentially no events having $\mu > 0$ occur and the motion is dominated by small creeping events with velocities of the order of the pulling speed. Standard parameters except that $s_2 = 100$. (a) Probability distribution, (b) time distribution of events, and (c) velocity as a function of position and time.

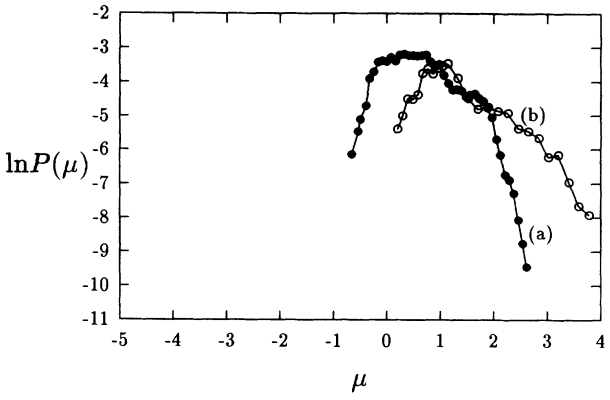

FIG. 8. Transition of dynamical motion to the regime where only large-scale events are seen. This transition occurs when either (a) dissipation parameter γ or (b) potential depth parameter k is increased substantially. For curve (a) $\gamma = 7.0$ and (b) $k = 800$. Other parameters are standard.

We notice that there is a large-event cutoff in the event probability distribution $P(\mu)$. The cutoff value is mainly determined by the parameter k. A larger k results in a larger maximum event size, since more energy is then stored in the system before it can be released. The effect of k on the maximum event size can be seen in Fig. 8. The maximum size is also affected by γ and by s_1, as can be seen in Figs. 8 and 5, because these parameters govern the total number of blocks involved in the largest events. As was discussed in Sec. IV B, this cutoff is not an effect of the finite size of the system.

D. Effects of minimum displacement $\Delta x_{\min}$ and pulling speed v

In a slipping experiment, it is important to exclude measurement noise from recorded events, so we set the criterion that a minimum displacement $\Delta x_{\min}$ would constitute a measured event. Any displacement (in a given time interval) smaller than $\Delta x_{\min}$ was ignored. In all the preceding calculations $\Delta x_{\min}$ was as defined in Eq. (8). Any decrease in $\Delta x_{\min}$ is expected to extend the probability distribution curve to the small-magnitude end, since smaller events are included. To verify that variation of $\Delta x_{\min}$ will not change the essential features of the event magnitude distribution we plot the distributions corresponding to three different $\Delta x_{\min}$ in Fig. 9. All three distributions were calculated using the same standard parameter set but with $\Delta x_{\min} = 1.5v\Delta t$, $2.0v\Delta t$, and $2.5v\Delta t$, respectively. A smaller $\Delta x_{\min}$ threshold, as expected, does give a probability function having an extended distribution in the small-event region. The slight decrease in the whole distribution curve for a small $\Delta x_{\min}$ is due to the renormalization of the probability function $P(\mu)$ following the increase in the total number of events. The scaling behavior and the structure of $P(\mu)$ are not changed by the change of threshold value $\Delta x_{\min}$. The crossover magnitude μ_0 is also invariant under this change. These results confirm that the threshold $\Delta x_{\min}$

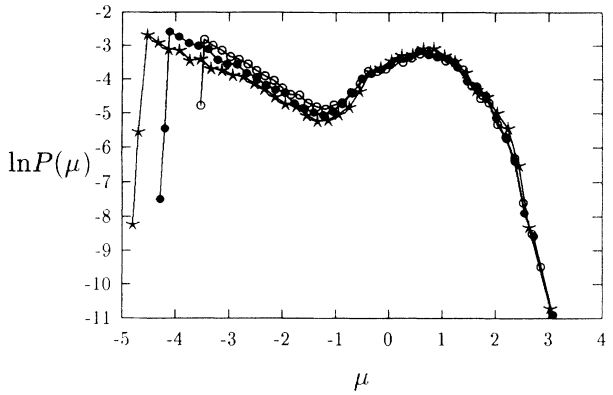

FIG. 9. Varying the minimum displacement $\Delta x_{\min}$ does not change the system's scaling behavior. All distributions have the standard parameters, and $\Delta x_{\min} = 1.5v\Delta t$ for open-circle curve, $2.0v\Delta t$ for filled-circle curve, and $2.5v\Delta t$ for star curve.

is acting as a measurement control quantity, and not as a system parameter.

The effect of changing the pulling speed is very similar to the effect of changing $\Delta x_{\min}$. Figure 10 compares probability distributions for three different pulling speeds with all other parameters being standard. They have the same distribution pattern, scaling behavior, and crossover magnitude as we have seen in the case of different thresholds $\Delta x_{\min}$. At lower pulling speeds, we see the distribution curve extend further into the small-magnitude end and a reduction in the small-event region. These reflect the fact that when the pulling speed is decreased smaller events are recorded, but also indicate that intermediate-size events increase in probability as the pulling speed is lowered. The crossover magnitude is again unchanged for different pulling speeds, as we can see from Fig. 10.

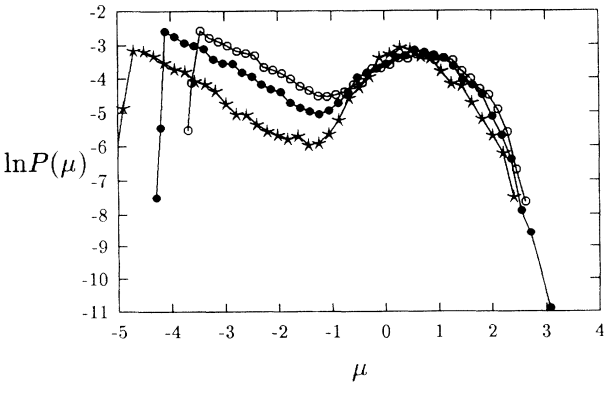

FIG. 10. The effect of changing the pulling speed v is similar to that of changing the threshold $\Delta x_{\min}$. While a lower speed creates additional smaller events, the dynamics of the system are not changed. For the curve with stars $v = 0.005$, the curve with filled circles $v = 0.015$, and for the curve with open circles $v = 0.03$. All other parameters are standard.

E. Boundary conditions and initial configuration

In systems in which long-range correlations occur it is important to verify that surface effects are not playing an unsuspected role in determining the system dynamics. In our model we used a chain of blocks and springs in which the ends were free. To see if these boundary conditions were causing any effects we performed calculations on systems with periodic boundary conditions for both $N = 50$ and $N = 100$. In contrast to the report in Ref. [1] that periodic boundary conditions tend to eliminate irregular motion and produce smooth, periodic solutions, we found almost identical results from the two kinds of boundary condition.

For the earthquake models with translational invariance, an irregular initial configuration like Eq. (7) is needed to produce stochastic slipping events exhibiting a wide range of magnitudes; otherwise a uniform initial configuration with every block in its equilibrium position will result in periodic solutions that only slowly diverge into irregular motion. This is not the case in our model. The random-depth potential causes uneven motion among blocks, with blocks at weaker potentials moving while others remain trapped in their positions. The independence of the results on the initial configuration was confirmed by numerical calculations with uniform initial configurations as in Eq. (6). The insensitivity of our model to boundary conditions and initial configurations makes it a robust model for studying stick-slip phenomena.

V. CONCLUSION AND DISCUSSION

We have proposed and studied a one-dimensional mechanical model for spatiotemporal dynamics. In contrast with some block-spring earthquake models, the friction between the blocks and the surface is not of the velocity-weakening type. Instead a random Gaussian potential and velocity-strengthening dissipation term are used to describe the static friction and viscosity. The model displays various slipping events with a wide range of magnitudes. These dynamics characteristic of self-organized criticality have been observed in our calculations for a wide range of model parameters.

The proposal and study of this model originated in work on chain pull-out in random copolymers. Its extension to a more general context was prompted by an experiment by Vallette and Gollub [5], in which those authors reported measurements whose results differed from the predictions of block-spring earthquake models. They noted that in their apparatus the friction was not velocity weakening but velocity strengthening, and that the scaling behavior of the event probability distribution did not always agree with earthquake models' predictions. The rubber-sheet system was found to cease its irregular behavior when the width of the sheet was substantially decreased. Results calculated from our model agree with these experimental data, and suggest that this model rep-

resents a new class of system exhibiting self-organized behavior. The model also seems to be a robust system for self-organized slipping in that the characteristic spatiotemporal dynamics do not depend on the size of system, boundary conditions, initial configurations, and pulling speed, or on the threshold that defines a minimal event.

ACKNOWLEDGMENTS

The authors are indebted to J. Gollub and D. Vallette for their comments on an earlier draft of this study. This work was supported by the National Science Foundation Materials Research Group program, and was funded by Grant No. DMR91-22227.

[1] J.M. Carlson and J.S. Langer, Phys. Rev. Lett. **62**, 2632 (1989); Phys. Rev. A **40**, 6470 (1989).
[2] J.M. Carlson, J.S. Langer, B.E. Shaw, and C. Tang, Phys. Rev. A **44**, 884 (1991).
[3] T.E. Tullis and J.D. Weeks, Pure Appl. Geophys. **124**, 383 (1986).
[4] J. Feder and H.J.S. Feder, Phys. Rev. Lett. **66**, 2669 (1991).
[5] D.P. Vallette and J.P. Gollub, Phys. Rev. E **47**, 820 (1993).
[6] H. Takayasu and M. Matsuzaki, Phys. Lett. A **131**, 244 (1988); M. Matsuzaki and H. Takayasu, J. Geophys. Res. **96**, 19 925 (1991).
[7] P. Bak, C. Tang, and K. Wiesenfeld, Phys. Rev. Lett. **59**, 381 (1987).
[8] R. Burridge and L. Knopoff, Bull. Seismol. Soc. Am. **57**, 341 (1967).
[9] J. Lomnitz-Adler, L. Knopoff, and G. Martinez-Mekler, Phys. Rev. A **45**, 2211 (1992).
[10] K. Chen, P. Bak, and S.P. Obukhov, Phys. Rev. A **43**, 625 (1991).
[11] L. Kadanoff, S.R. Nagel, L. Wu, and S. Zhou, Phys. Rev. A **39**, 6524 (1989); H.M. Jaeger, C. Liu, and S.R. Nagel, Phys. Rev. Lett. **62**, 40 (1989).
[12] G.A. Held, D.H. Solina, D.T. Keane, W.J. Haag, P.M. Horn, and G. Grinstein, Phys. Rev. Lett. **65**, 1120 (1990).
[13] G.L. Vasconcelos, M. de Sousa Vieira, and S.R. Nagel, Physica A **191**, 69 (1992).
[14] L. Knopoff, J.A. Landoni, and M.S. Abinante, Phys. Rev. A **46**, 7445 (1992).
[15] B. Guterberg and C.F. Richter, Ann. Geofis. **9**, 1 (1956).

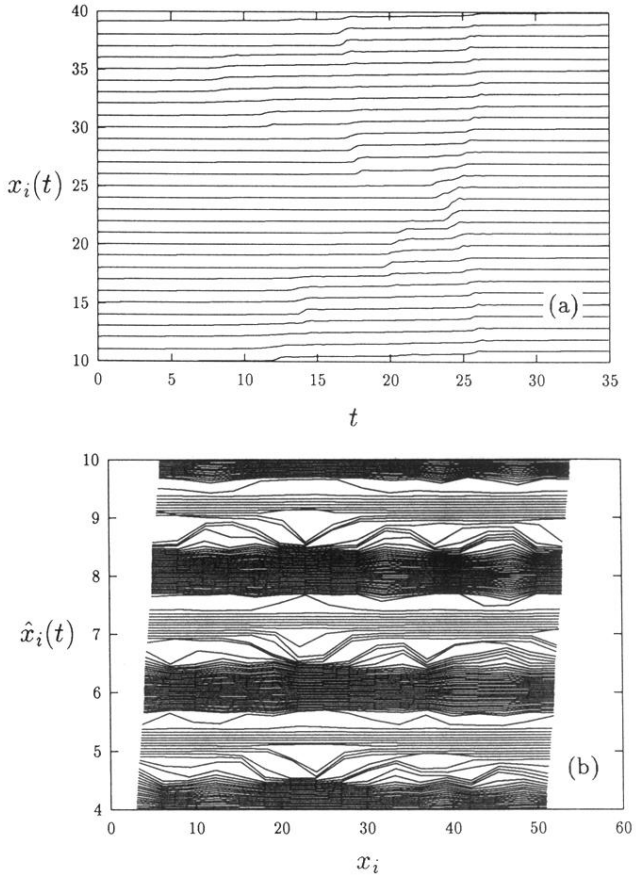

FIG. 2. The model shows a wide range of slipping events. Shown here is a typical system with parameters $s_1 = 30$, $s_2 = 20$, $k = 350$, $d = 50$, $v = 0.015$, and $\gamma = 4.0$. (a) Displacement of blocks as a function of time, (b) equal-time contour map showing the cumulative displacement $\hat{x}_i(t)$ as a function of position and time.

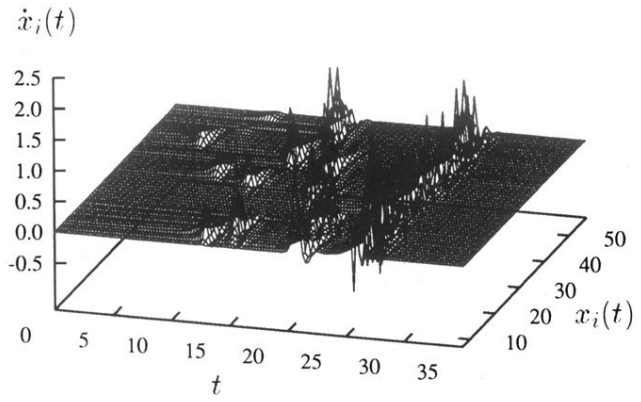

FIG. 3. In this replotting of the data of Fig. 2, the velocities of blocks are shown as a function of position and time. Both localized events with small velocities and big events with large velocities are seen.

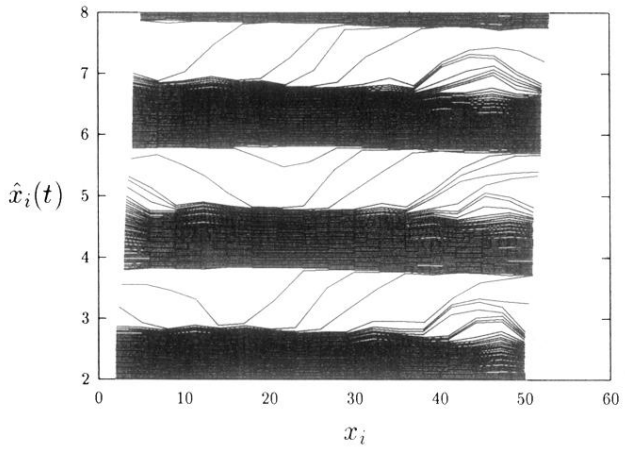

FIG. 6. Cumulative displacement for a system with strong dissipation. Parameters are the same as for the flatter curve in Fig. 5(a). Few small events are visible, and the system is predominantly in either the stuck or the large-slipping state.

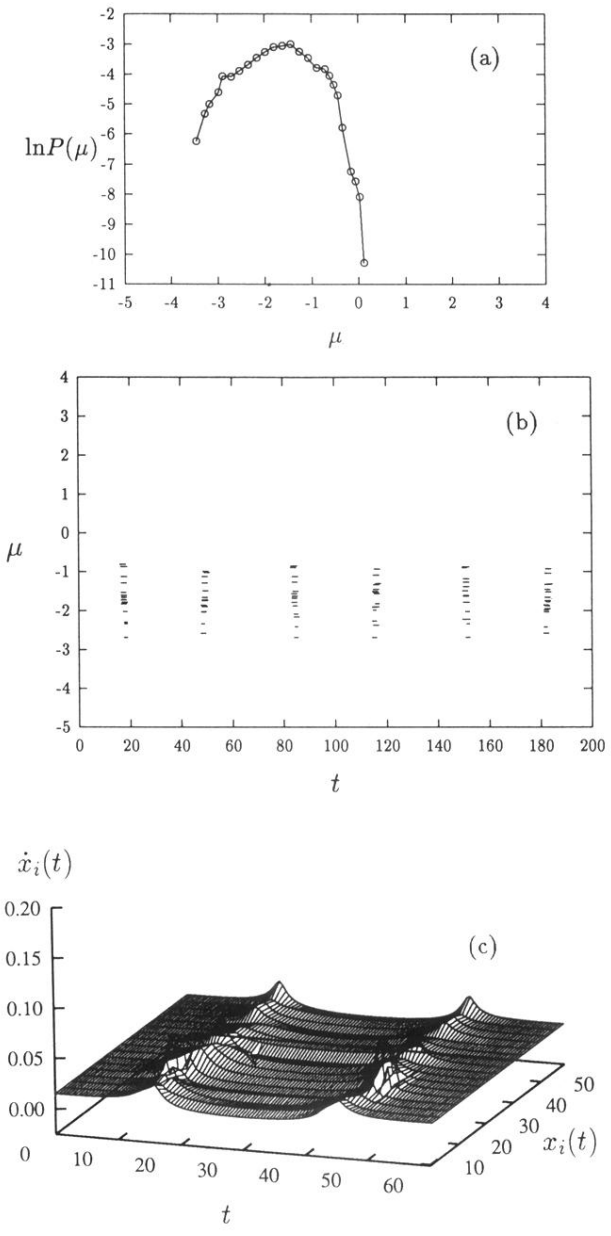

FIG. 7. System loses instability when the parameter s_2 is sufficiently large. Essentially no events having $\mu > 0$ occur and the motion is dominated by small creeping events with velocities of the order of the pulling speed. Standard parameters except that $s_2 = 100$. (a) Probability distribution, (b) time distribution of events, and (c) velocity as a function of position and time.